CrossMark

Research Article

Composite Microparticles Based on Natural Mucoadhesive Polymers with Promising Structural Properties to Protect and Improve the Antifungal Activity of Miconazole Nitrate

G. Tejada,[1] M. C. Lamas,[1,2] M. Sortino,[3,4] V. A. Alvarez,[5,6] and D. Leonardi[1,2,6]

Abstract. Oropharyngeal candidiasis is a recurrent oral infection caused by *Candida* species. Gel formulation containing miconazole nitrate is the most common approach for treating oral candidiasis. However, traditional oral topical antifungal therapies have many limitations, including short contact time with the oral mucosa and the necessity to administrate various doses per day. Thus, the aim of this work was to formulate composited microparticulated systems based on combinations of mucoadhesive cationic, anionic, and nonionic polymers that could protect and modify the drug release rate and therefore avoid a fast dilution of the drug by saliva. Microparticulated systems were prepared by the spray drying method employing chitosan, gelatin, and hydroxypropyl methylcellulose. The morphology of the systems was investigated by scanning electron microscopy; drug crystallinity was studied by X-ray, while interactions between polymers were analyzed by infrared spectroscopy. Drug release and halo zone test were employed to analyze the release and activity of the systems loaded with miconazole against *Candida albicans* cultures. The most appropriate microparticulated system was the one based on chitosan and gelatin which showed homogeneous morphology (mean size of 1.7 ± 0.5 μm), a protective effect of the drug, and better antifungal effect against *Candida* culture than miconazole nitrate and the other assayed systems. Taking into account these results, this approach should be seriously considered for further evaluation of its safety and *in vivo* efficacy to be considered as an alternative therapeutic system for the treatment of oral candidiasis.

KEY WORDS: antifungal; composite microparticles; chitosan; gelatin; hydroxypropyl methylcellulose; thermal protective effect.

INTRODUCTION

Candida albicans is the most important fungal opportunistic pathogen. It usually resides as a commensal in the gastrointestinal and genitourinary tracts and in the oral and conjunctival flora and causes infection when the host becomes debilitated or immunocompromised [1]. Immunocompromised patients, including individuals infected with human immunodeficiency virus, who have undergone chemotherapy, or received organ transplants, are highly susceptible to the development of candidiasis [2]. Oropharyngeal candidiasis is a recurrent oral infection caused by *Candida* species. Traditional oral topical antifungal therapies have many limitations, including short contact time with the oral mucosa and the necessity to administrate various doses per day. Miconazole nitrate (MN) is an antifungal drug used to treat topical fungal and yeast infections. Gel formulation containing 2% of MN is the most common approach for treating oral candidiasis. However, it has to be applied four times a day after meals due to the rapid clearance of the drug from the oral mucosal surfaces, because of the movement of the tongue and jawbones, and because of the continuous dilution of the drug by saliva [3,4]. Therefore, drug inclusion into a mucoadhesive formulation is desirable in order to achieve prolonged mucosal contact and higher drug concentration

[1] IQUIR-CONICET, Suipacha 570, 2000, Rosario, Argentina.
[2] Área Técnica Farmacéutica, Departamento Farmacia, Facultad de Ciencias Bioquímicas y Farmacéuticas, Universidad Nacional de Rosario, Suipacha 570, 2000, Rosario, Argentina.
[3] Área Farmacognosia, Departamento Química Orgánica, Facultad de Ciencias Bioquímicas y Farmacéuticas, Universidad Nacional de Rosario, Suipacha 570, 2000, Rosario, Argentina.
[4] Centro de Referencia de Micología (CEREMIC), Facultad de Ciencias Bioquímicas y Farmacéuticas, Universidad Nacional de Rosario, Suipacha 570, 2000, Rosario, Argentina.
[5] Grupo de Materiales Compuestos Termoplásticos (CoMP), Instituto de Investigaciones en Ciencia y Tecnología de Materiales (INTEMA, CONICET-UNMdP), Av. Colón 10890, 7600, Mar del Plata, Argentina.
[6] To whom correspondence should be addressed. (e-mail: alvarezvera@fi.mdp.edu.ar; leonardi@iquir-conicet.gov.ar)

on the oral mucosal surface. In this context, during the last years, films [5,6], tablets [7,8], and microparticulated systems [9,10] have been investigated with the aim of enhancing the efficacy of topic medications, by prolonging the contact time between the drug and the oral mucosal surface. Particularly, bioadhesive microparticles based on chitosan (CH) have been developed and employed for the delivery of fluoride in the mouth to sustain fluoride retention in the oral cavity and to provide increased protection against caries [11]. Recently, solid lipid microparticles loaded with doxycycline hydrochloride-metronidazole have been developed and tested, *in vitro* and *in vivo*, for the treatment of periodontitis [12]. Additionally, microparticles/discs of betamethasone for the management of oral *lichen planus* were developed and characterized [13]. Cartagena *et al.* have developed MN microparticulated systems based on synthetic polymers Eudragit L-100 and Gantrez MS-955 [14], the microparticles were characterized, and the antifungal assay demonstrated that MN-loaded microparticles provided the same anti-*Candida albicans* activity of the raw drug. Later, in 2017, a new denture adhesive containing MN polymeric microparticles based on Eudragit L-100 and Gantrez MS-955 has been developed by Cartagena *et al.* [15]. The denture adhesive showed effective antifungal activity, good adhesive force, and low or no toxicity properties. Both polymers employed in these works were synthetic and did not present antifungal activity by themselves. CH is the deacetylated derivative of chitin, which proved to be adhesive and acts as a natural antimicrobial compound even against *C. albicans* [16–18]. This polymer has been used to produce microparticles loaded with different active compounds improving the dissolution rate and activity of several poor water-soluble drugs [19–22], or used as sustained drug delivery system. Combinations of positively charged CH and other polymers can significantly alter several properties of drug delivery systems, including their morphology, drug encapsulation efficiency, and drug release kinetics [17,23]. For example, the combination of CH, sodium alginate, and pectin has modified the release of the loaded compounds from the particles depending on the pH media [24]. On the other hand, nonionic and anionic polymers also have been employed to formulate drug delivery systems [25,26]. Recently, microparticles based on hydroxypropyl methyl cellulose (HPMC), a nonionic polymer, were used to formulate a vancomycin hydrochloride-controlled release system [27], while microparticles based on gelatin (GEL), an anionic polymer, were loaded with cinnamoyl modifying the drug release with the pH of the medium [28]. Microparticles based on CH loaded with MN may increase its antifungal activity with respect to the free drug due to the polymer antimicrobial activity [29,30]. Additionally, microparticles based on combinations between different biodegradable polymers could modify the MN release rate and therefore avoid a fast dilution of the drug by saliva.

In the case of biodegradable polymer systems or formulation, it is important to select appropriate techniques of characterization such as X-ray diffraction (a powerful nondestructive technique to identify crystalline structures) and thermoanalytical methods, such as thermogravimetric analysis (TGA) and differential scanning calorimetry (DSC) to determine the thermal characteristics (glass transition, melting, and degradation temperatures) [31].

Thus, the aims of this work were to formulate and to characterize polymeric microparticulated systems loaded with MN as alternative therapeutic systems for the treatment of oral candidiasis, particularly by formulating systems based on combinations of natural cationic (CH), anionic (GEL), and nonionic (HPMC) polymers.

MATERIALS AND METHODS

Materials

CH (230 kDa average molecular weight and 80.6% of N-deacetylation) was supplied by Aldrich Chemical Co. (Milwaukee, WI, USA), and HPMC (MW 250 kDa, methoxyl content 19–24%, hydroxypropyl content 7–12%, K4M grade) was purchased from Eigenmann & Veronelli (Milan, Italy). GEL (type A from pork skin, 125 Bloom grams) and miconazole nitrate pharmaceutical grade were purchased from Parafarm (Buenos Aires, Argentina). All other chemicals were of analytical grade.

Methods

Preparation of Microparticles

CH solutions (0.1% *w/v*) were prepared by dissolving CH in a solution of 30% *v/v* acetic acid (pH = 2.50), while GEL and HPMC solutions (0.1% *w/v*) were obtained by dissolving them in distilled water. Polymeric solutions were mixed by stirring at 400 rpm for 30 min and 40°C. After that, MN 70% *w/w* (considering the mass of the polymers) was added and stirred (400 rpm, 10 min, 40°C). Then, the final mixtures were fed to the nozzle *via* a peristaltic pump using a Buchi Mini dryer B-290 (Flawil, Switzerland). The following parameters remained constant: airflow rate of 38 m^3/h, feed rate of 5 mL/min, aspirator at 95%, spray drying inlet temperature of 130°C, and outlet temperature of 70°C. After spray drying, the powders were removed from the collector vessel and stored at room temperature. For the preparation of unloaded microparticles, without MN, the same procedure was employed.

Finally, the systems were compressed to obtain the microparticles/discs using a Beckman press (8 tons for 10 min).

Encapsulation Efficiency

Encapsulation efficiency (EE) was determined by dissolving 30 mg of each sample in 90 mL methanol. The suspension was incubated, for 4 h, at room temperature under magnetic stirring (400 rpm) in order to extract the drug. The amount of MN in each sample was determined spectrophotometrically by measuring the absorbance at 272 nm using a LKB-Pharmacia Ultrospec II spectrophotometer (Cambridge, UK). The concentrations of MN were obtained using

a calibration curve, and this method was previously validated. The EE% was calculated according to Eq. (1):

$$EE\% = \frac{W_{MN}}{W_t} \times 100\%$$
(1)

Where W_{MN} is the actual MN content and W_t is theoretical MN content in the microparticles. Each experiment was performed in triplicate.

Dissolution Studies

Dissolution studies were performed in 900 mL of distilled water containing 1% *v/v* PEG 400 at 37°C, using a USP XXIV Apparatus 2 (Paddle Apparatus) (Hanson Research, SR8 8-Flask Bath, Ontario, Canada) with paddles rotating at 50 rpm [5,6]. Different masses of microparticles (equivalent to 200 mg MN) were dispersed in the dissolution medium. At different time intervals—0, 10, 20, 30, 40, 50 60, 90, 120, 180, 240, and 300 min—three samples of 5 mL each were taken using a 0.45-μm filter. The amount of drug released was determined by UV spectrophotometry using the absorption band of the drug at 272 nm. An equal volume of the dissolution medium was added after each sample collection to maintain a constant volume.

In Vitro Residence Time

The *in vitro* residence time was determined using a modified USP disintegration apparatus. The disintegration medium consisted of 900 mL artificial saliva maintained at 37°C. A segment of porcine gum (obtained from "Paladini" slaughterhouse, V.G. Galvez, Argentina), 3 cm long, was glued to the surface of a glass slab, vertically attached to the apparatus. Each mucoadhesive microparticle/disc was hydrated from one surface using 0.1 ml of artificial saliva and then the hydrated surface was brought into contact with the mucosal membrane. The glass slab was vertically fixed to the apparatus and allowed to move up and down so that the microparticle/disc was completely immersed in the solution at the lowest point and was out at the highest point. The time necessary for complete erosion or detachment of each microparticle/disc from the mucosal surface was recorded [32–34]. The results presented are mean values of three determinations.

Morphology Analysis and Size Determination by Scanning Electron Microscopy

Morphology and particle size of raw MN and microparticles were investigated by scanning electron microscopy (SEM, AMR 1000, Leitz, Wetzlar, Germany). Systems powders were mounted on an aluminum sample support by means of a conductive and double-sided adhesive. The samples were coated with a fine gold layer for 15 min at 70–80 mTorr in order to make them conductive before obtaining the SEM micrographs. All samples were examined using an accelerating voltage of 20 kV and magnification of ×10,000. SEM images were analyzed using the Image-Pro Plus (IPP)

software v. 6.0 to determine an indirect estimation of the particle size. About 200 crystal Feret's diameters were considered in each particle size distribution calculation [35].

Fourier-Transform Infrared Spectroscopy

Fourier-transform infrared spectra of MN, polymers, and loaded and empty microparticles were obtained by a FT-IR-Prestige-21 Shimadzu spectrometer (Tokyo, Japan) at room temperature, using attenuated total reflectance with ZnSe crystal (ATR) for the sample analyses. Scanning range was 400–4000 cm^{-1} (10 scans) with a resolution of 1 cm^{-1}.

Thermal Analysis

TGA was performed with a TG HI-Res thermal analyzer (TA Instruments) at a heating rate of 10°C/min from room temperature to 800°C in air flow.

DSC tests were performed in a DSC Q2000 (TA Instruments) from −25 to 250°C at a heating rate of 10°C/min under nitrogen.

X-Ray Diffraction

Data collection was carried out in transmission mode on an automated X'Pert Philips MPD diffractometer (Eindhoven, The Netherlands). X-ray diffraction patterns (XRD) were recorded using CuKα radiation ($\lambda = 1.540562$ Å), a voltage of 40 kV, a current of 20 mA, and steps of 0.02° on the interval $2\theta = 10–50°$. Low peak broadening and background were assured by using parallel beam geometry by means of an X-ray lens and a graphite monochromator placed before the detector window. Data acquisition and evaluation were performed with the Stoe Visual-Xpow package, Version 2.75 (Germany).

Halo Zone Test

Halo zone test was performed following the guidelines of disk diffusion method described in CLSI document M44-A2 [36]. *C. albicans* (ATCC 10231) was cultured in Sabouraud's dextrose agar 24 h before testing. Testing was carried out on agar plates (150 mm diameter) containing Mueller-Hinton agar, supplemented with 2% glucose (2 g/100 mL) and 0.5 μm/mL methylene blue, at a depth of 4.0 mm. The inoculants were prepared by suspending five distinct colonies in 5 mL of sterile distilled water and shaking on a vortex mixer for 15 s. The agar surface was inoculated by dipping sterile cotton swabs into a cell suspension adjusted to a turbidity of a 0.5 McFarland standard (approximately 1–5$10^6$ CFU/mL) and by streaking the plate surface in three directions.

The plate was allowed to dry for 20 min, then the MN powder (1000 μg) was used as control, and microparticles/discs (mass equivalent to 1000 μg MN) were placed attached to a Scotch tape onto the surface of the agar. Each Scotch tape was moved to another zone of the culture after 1 h and the procedure repeated for 7 h. After that, the plates were incubated in air at 28°C and read after 24 h. Halo diameters (in millimeters) for the zone of complete inhibition were

determined using a caliper, and the mean value for the organism was recorded [6].

Statistical Analysis

Analysis of variance was used, and when the effect of the factors was significant, the Tukey multiple ranks honestly significant difference test was applied (GraphPad Prism 5). Differences at $p < 0.05$ were considered significant.

RESULTS AND DISCUSSION

The pH values of the different polymeric solutions were 2.49 (CH), 5.81 (GEL), and 5.66 (HPMC). These pH values indicate that chitosan carries a positive charge and can interact with gelatin that carries a negative charge due to the ionization of its carboxylic groups. As it can be observed in Table I, the EE% was higher than 80% when at least one of the polymers employed was charged (cationic or anionic), while microparticles prepared with HPMC showed reduced values of EE% (75%). These results could be probably related to the fact that polymers showing high charge density have more sites to interact with MN when both the drug and the polymer are in solution, before the spray drying process [37]. Thus, when solutions are sprayed, those having more interacting groups are able to load more MN inside the formed particles. The highest EE% was obtained when just one charged polymer was employed to prepare the micro-particles (97.8 and 98.5% for CH and GEL, respectively), while EE% decreased when the two charged polymers were combined (83.2% for CH-GEL). This decrease is probably related to the interactions between positive charges present in CH and negative charge densities present in GEL; thus, a minor quantity of charge densities is available to interact with MN and to maintain the drug into the polymeric blend. The mentioned behavior could also explain the MN released rate from the systems (Fig. 1). Microparticles based just on HPMC showed the fastest drug release, reaching almost 100% after 30 min (Table I, Fig. 1). Oppositely, systems based just on GEL or CH released lower amounts of MN—10.2 and 13.2% of MN, respectively, while systems based on combinations of polymers showed releases in the range between 35 and 44% after 30 min assay. Among them, the matrix based on both charged polymers showed the slowest drug release rate. It is important to note that all systems improved the dissolution rate of the free MN ($Q_{30} = 1.4\%$). Several factors could be responsible for this fact, and among them is the reduction of

MN crystallinity during the spray drying process and/or the enhancement of wettability due to contact with the polymeric matrix [38]. All microparticles/discs showed adhesiveness, presenting *in vitro* residence times higher than 1.5 h (Table I). The systems based on CH-HPMC and CH-GEL did not detach or disintegrate after 8 h assay. On the other hand, microparticles/discs based on CH and HPMC were detached without disintegration after 6 and 5 h, respectively, while those based on GEL and HPMC-GEL disintegrated after 1.5 and 3 h, respectively.

Regarding morphology and size (reported in Table I and Fig. 2), it can be observed that MN appears as regular crystalline blocks, which ranged in size from 0.5 to 11 μm and showed an average size of 3 μm (Fig. 2a), while microparticulated systems ranged from 0.4 to 5 μm (Fig. 2b–g).

Microparticles based on CH (Fig. 2b) presented a smooth and shrunk surface (size range from 0.2 to 3.2 μm), similar to microparticles based on GEL (size range from 0.5 to 4 μm, Fig. 2c), whereas microparticles based only on HPMC (size range from 2.2 to 5.0 μm) were irregular and fibrous with nonuniform surface (Fig. 2d). In the case of microparticles based on polymer combinations, HPMC-GEL (Fig. 2g) showed a nonuniform shrunk surface and irregular shape (size range from 1.0 to 5.5 μm). On the other hand, particles based on CH-GEL (size range 0.8 to 3.2 μm) and CH-HPMC (size range 0.4 to 2.8 μm) were smooth and spherical showing uniform surface (Fig. 2e, f).

Fourier-Transform Infrared Spectroscopy (FTIR)

As it can be observed in Fig. 3, MN presents characteristic bands at 3474 cm^{-1} (hydroxyl groups), 3178 and 3107 cm^{-1} (aromatic C–H stretch vibrations), 2828 and 1473 cm^{-1} (aliphatic C–H stretch and C–H bending), 1921 and 1587 cm^{-1} (C–C stretching), 1329 cm^{-1} (NO$_2$ bending), 1310 cm^{-1} (C–N stretching), 1087 cm^{-1} (C–O–C stretching), 1041 and 1010 cm^{-1} (aromatic C–H bending), and 824 and 712 cm^{-1} (C–Cl group stretch vibrations) [39,40].

All microparticulated systems loaded with MN showed the MN characteristic peaks at 1587, 1329, 1310, 1087, 1041, 1010, 824, and 712 cm^{-1} with slight shifting with respect to the MN raw material confirming the presence of the loaded drug (Fig. 3). Regarding the spectra of polymers, it can be see that the CH spectrum showed several bands at 3450 cm^{-1} (stretching vibration of O–H and N–H groups associated by intra- and intermolecular hydrogen bonding), 2925 cm^{-1}

Table I. Properties of the Studied Microparticulated Systems

| Systems	EE (%)	Q_{30} (%)	Morphology	Mean size (μm)	*In vitro* residence time (min)
MN	–	1.4	Crystalline blocks	3.0 ± 2.0	–
CH-MN	97.8	13.2	Spherical, smooth, shrunk surface particles	2.1 ± 0.4	360
HPMC-MN	74.4	99.9	Coalesced, irregular, fibrous particles	3.9 ± 0.9	300
GEL-MN	98.5	10.2	Coalesced, irregular particles	1.9 ± 0.6	90
CH-HPMC-MN	82.4	44.5	Spherical particles	1.4 ± 0.4	>480
CH-GEL-MN	83.2	35.6	Spherical particles	1.7 ± 0.5	>480
HPMC-GEL-MN	94.9	41.9	Irregular, shrunk, nonuniform surface particles	3.1 ± 0.9	180

Q_{30}, percent of MN dissolved at 30 min
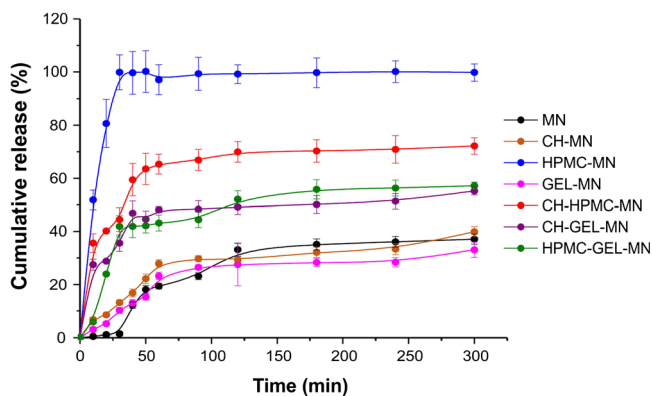
Fig. 1. Dissolution profiles of MN and different systems assayed

(stretching vibration of the C–H), 1643 cm^{-1} (amide I), 1595 cm^{-1} (NH$_2$ bending), 1420 cm^{-1} (stretching vibration of the carboxylic acid salt COO$^-$), and 1173 cm^{-1} (amino groups). The GEL spectrum showed bands at 1680 cm^{-1} (COO$^-$ stretching vibration), 1640 cm^{-1} (amide I band), and 1535 cm^{-1} (amide band II). Finally, the HPMC spectrum showed bands at 3450 cm^{-1} (O–H stretching), 1653 and 1635 cm^{-1} (stretching vibration C–O for six-member cyclic rings), and 1458 cm^{-1} (C–O–C stretching of cyclic anhydrides).

When CH was combined with HPMC, the obtained spectra were overlapping on the polymers without shifting of any original peak or appearance of new bands, and this overlapping indicates no strong interactions between polymers (Fig. 4). Similar results were obtained when the combination GEL-HPMC was analyzed. On the other hand, several shifts and new infrared bands were observed in the case of the combination CH-GEL. The spectrum showed that the amide I peak was shifted from 1640 to 1652 cm^{-1} and the NH$_3^+$ band and asymmetric and symmetric COO$^-$ stretching vibration at 1600 and 1420 cm^{-1} disappeared, indicating an electrostatic interaction between the amine groups of CH (NH$_3^+$) and carboxyl groups (COO$^-$) of GEL (Fig. 4). Additionally, the appearance of a strong band at 1550 in the CH-GEL spectrum could be due to electrostatic interactions between the COO$^-$ group of GEL and the NH$_3^+$ group of CH [41,42].
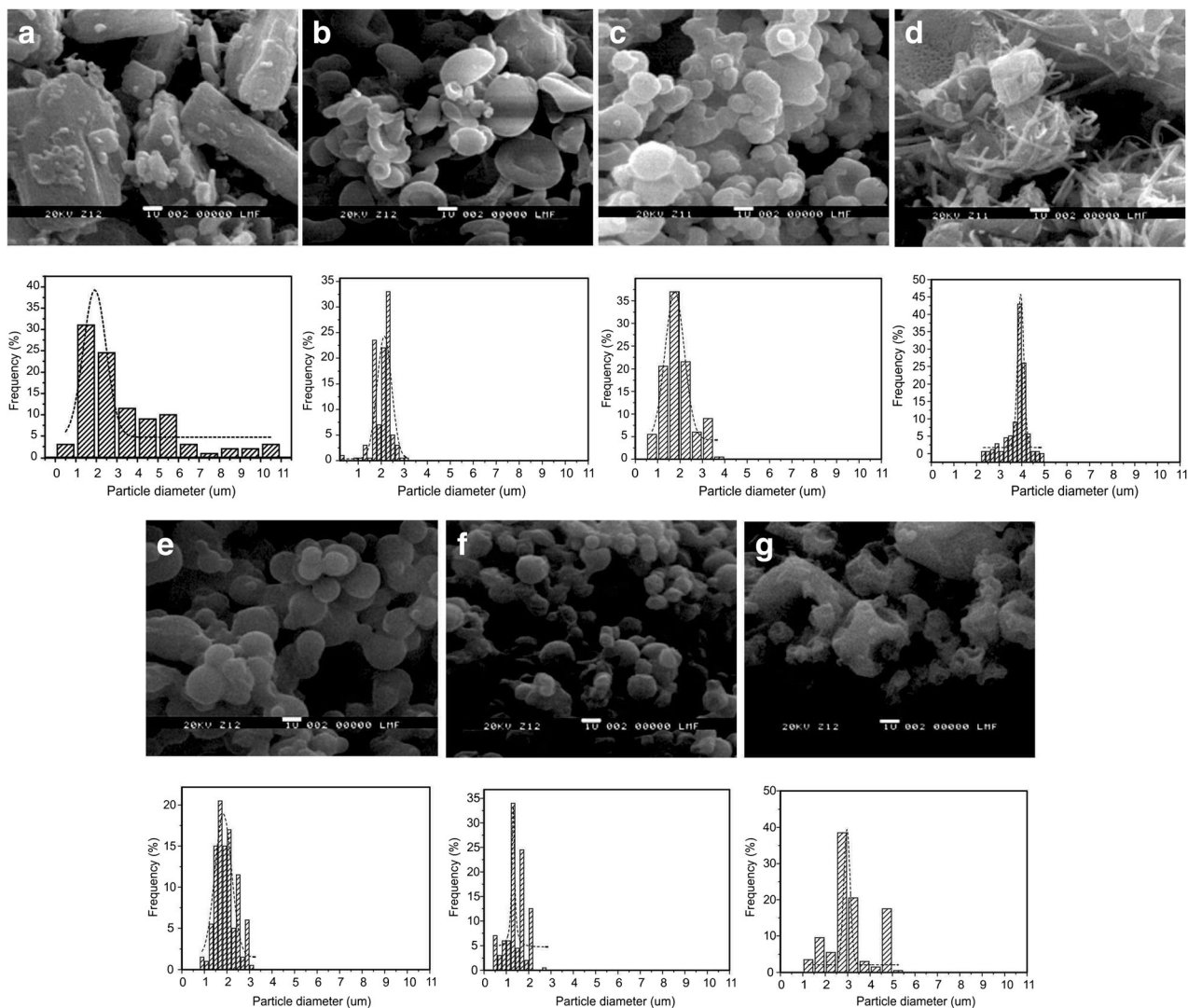

Fig. 2. SEM images and particle size histogram of the drug (**a**) and loaded microparticles (**b–g**): **a** MN, **b** CH, **c** GEL, **d** HPMC, **e** CH-GEL, **f** CH-HPMC, and **g** HPMC-GEL
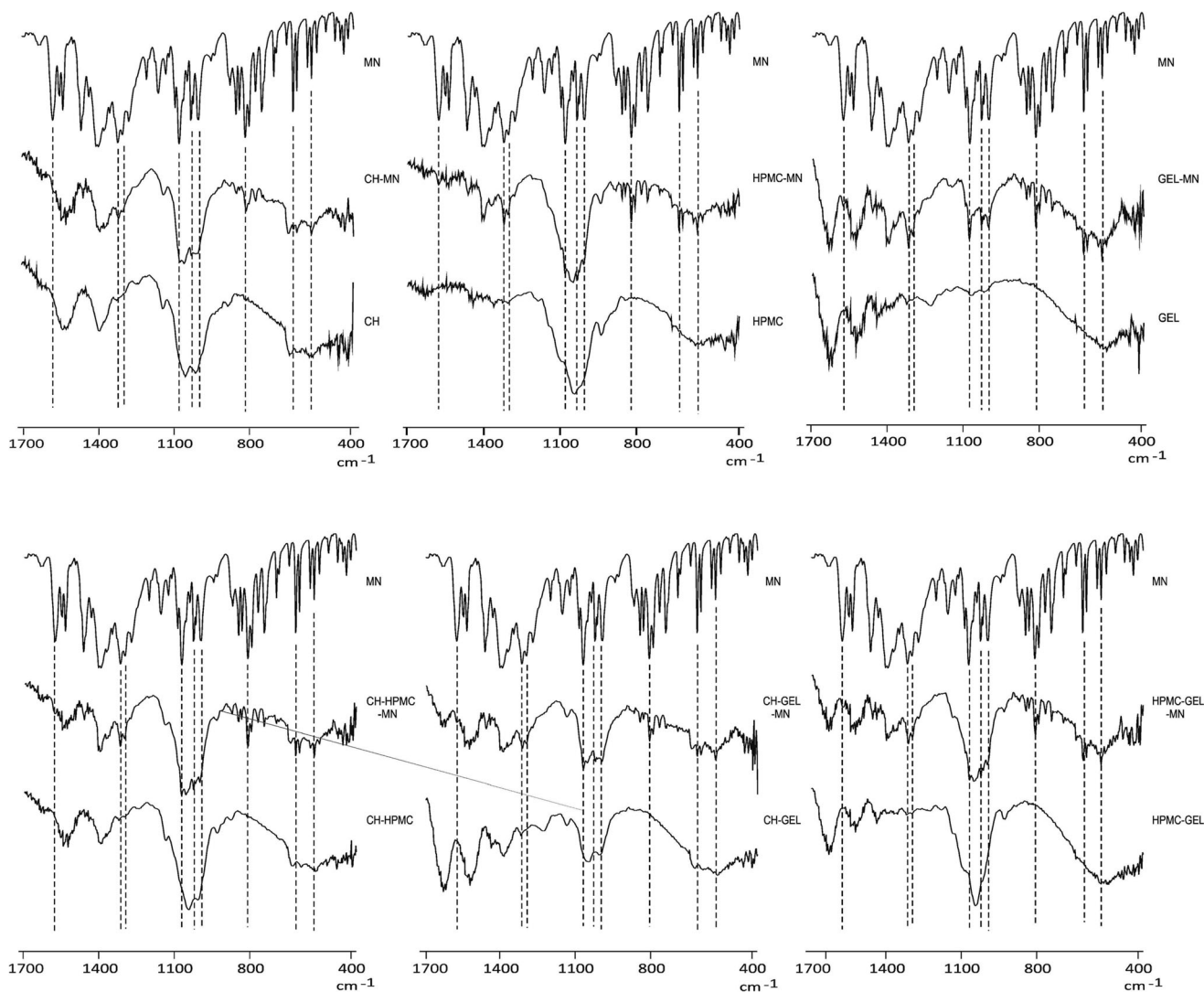
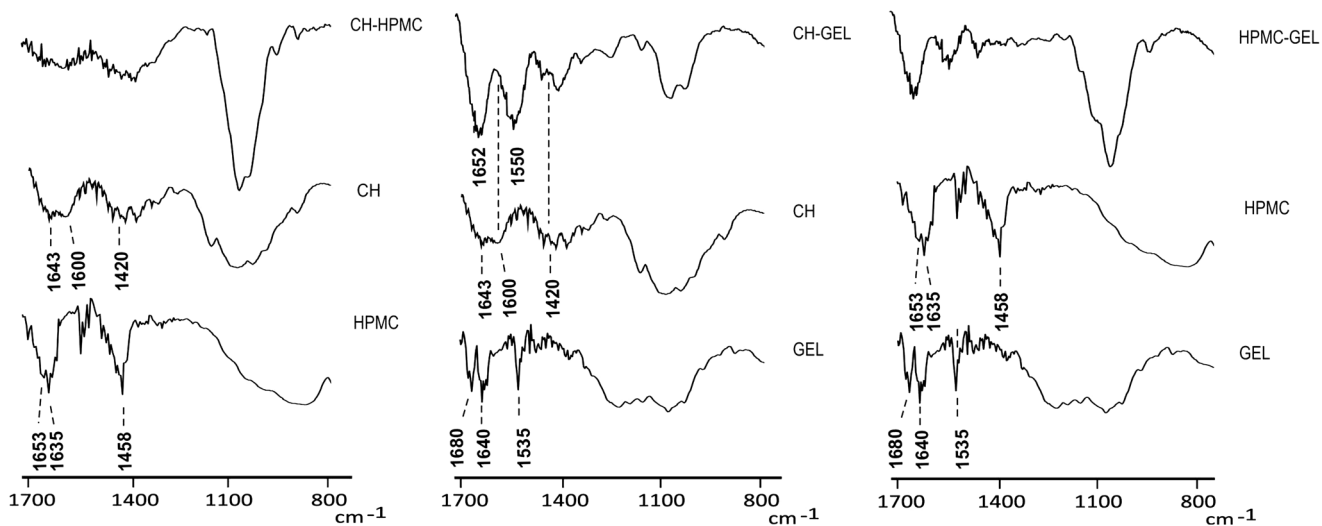**Fig. 3.** Infrared spectra of MN, polymers, and loaded and unloaded microparticles

Fig. 4. Infrared spectra of CH, HPMC, GEL, and microparticles based on polymer combinations

Thermal Characterization

Figures 5 and 6 show the TGA and DTGA (derivate of TGA curves) curves of the studied systems, respectively. TGA and DTGA indicated that the CH polymer degraded in a single stage at 292°C corresponding to its depolymerization [43]. A small peak, related to the water absorbed, between 40 and 100°C can also be observed; it corresponds to the first mass drop in the TGA curve [43]. In addition, the unloaded microparticles present two peaks of degradation: one centered at 126°C and the other close to 275°C. While the former could be associated with water within the material, the latter corresponds to the depolymerization of CH. As it is commonly observed in microencapsulated systems, the process of capsule manufacturing produces a reduction in thermal stability with respect to the polymer alone; in this case, the reduction is around 17°C [44]. The fact that the thermal decomposition of empty microparticles has begun at lower temperature than that of the pure polymer can be related to the fact that microparticles when exposed to thermal degradation their micrometric size makes the superficial area larger compared with the polymer, and since the microparticles are exposed to a wider superficial area, they are degraded more easily [44]. Regarding the drug MN, it has a broad peak centered at 309°C with a shoulder around 200°C; in the case of the microparticles of CH loaded with the drug, three peaks, centered at 134, 250, and 270°C, respectively, can be detected in the DTGA curves. The first peak corresponds to water associated with the material [43], the second is associated with the drug, and finally, the third is a combination between the drug and the CH used as vehicle.

The HPMC polymer presents degradation in a single stage whose maximum degradation is centered at 350°C [45].

It can also be observed that the empty microparticles present one degradation peak centered at around the same temperature as the polymer (350°C). In the case of the microparticles of HPMC-MN, it is possible to observe two peaks, centered at 267 and 350°C, and one shoulder, at around 200°C, in the DTGA curves. Both the shoulder and the first peak can be associated with MN, whereas the last is associated with HPMC used as vehicle [45]. On the other hand, the GEL polymer degraded in a single stage exhibited a peak centered at 325°C [46,47]. In addition, a little peak near to 67°C can be associated with the evaporation of water. In this case, the unloaded microparticles present one degradation peak centered at a lower temperature than the neat polymer (316°C), as it is common in microencapsulated systems [44]. In the case of the microparticles of GEL loaded with the drug, two peaks, centered at 275 and 325°C, respectively, and one shoulder, at around 200°C, can be observed in the DTGA curves. Once again, the shoulder and the first peak can be associated with MN, whereas the last one can be related to the polymer used as vehicle [46,47]. In the case of the microparticles of CH-HPMC loaded with MN, it is possible to observe four peaks centered at 92.3, 242.1, 275.4, and 342.1°C, respectively, in the DTGA curves. The first peak corresponds to water associated with the material, the second is associated with a combination between the drug and CH [43], the third is a combination between the drug and both polymers used as vehicle, and the last one is associated with the HPMC polymer [45]. Similar results regarding the degradation of each polymer, the drug, and empty and loaded microparticles (MPs) were observed for the CH-GEL and GEL-HPMC systems.

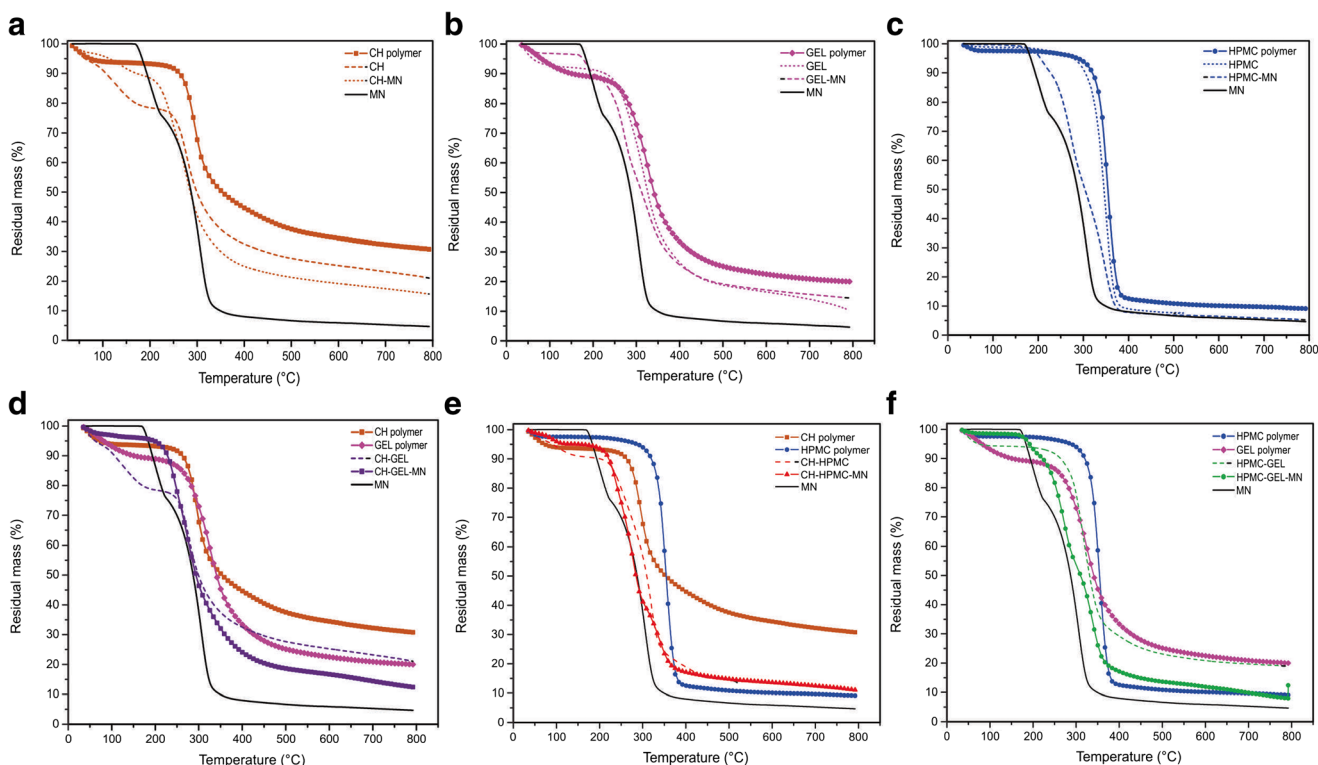The melting temperatures of each study obtained from DSC are summarized in Table II. for Tm of the empty

Fig. 5. TGA curves of the studied systems: **a** CH, **b** GEL, **c** HPMC, **d** CH-GEL, **e** CH-HPMC, and **f** HPMC-GEL
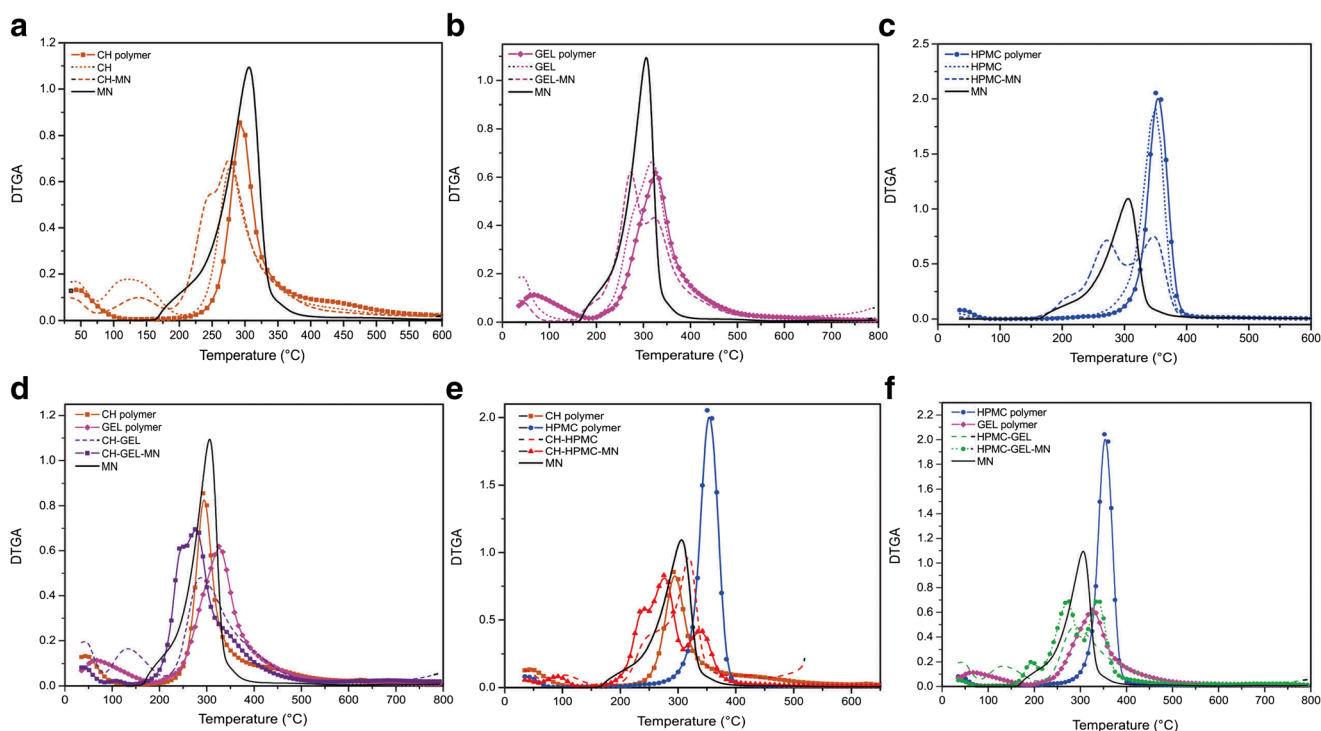
Fig. 6. DTGA curves of the studied systems: **a** CH, **b** CH-HPMC, **c** HPMC, **d** GEL, **e** CH-GEL, and **f** HPMC-GEL

particles (without MN) are also included. The endothermic peak for MN was centered at 186.1°C, whereas for the neat polymers, the peaks were 189.5°C (CS), 194.4°C (HPMC) and 184.9°C (GEL).

In the case of the polymers (CH, HPMC, and GEL), a first peak (around 130–150°C) related with water was observed, whereas in each system, the peak at a higher temperature can be associated with the melting of each polymer [48–50]. In the case of MN, only the melting of the drug was observed.

It can be also observed that in all the studied systems, the DSC curve of the drug-containing microparticles shows the event corresponding to the melting of the corresponding polymers. In addition, the microencapsulation process did not affect the polymer structure because the pure polymer presented similar values for relaxation enthalpy. DSC curves did not detect any crystalline drug material in the MN-loaded microparticles; the endothermic peak of MN was absent or it was not detectable. Thus, it can be postulated that the drug incorporated into the microparticles was in an amorphous or disordered crystalline phase of a molecular dispersion or a solid solution state in the polymeric matrix [51]; this result will be confirmed by XRD studies.

X-Ray Diffraction

XRD was carried out to confirm the results of the thermogravimetric studies and to complete the characterization of the microparticles/discs. Figure 7 shows the X-ray patterns of the MN raw material, polymers, and different formulations. The diffractograms of raw materials were in agreement with previously reported data. The MN spectra showed sharp and narrow peaks at diffraction angles (2θ): 13.05°, 14.49°, 15.59°, 16.22°, 18.55°, 20.80°, 21.57°, 22.95°,

25.19°, 26.15°, 27.32°, 29.9°, 31.82°, 33.12°, 36.6°, and 40.69°, with a typical crystalline pattern [40]. The raw CH showed a peak at 20° related to the anhydrous CH crystals [52]. The GEL only had a typically wide crystalline peak at 21.8° [53], while the HPMC presented two peaks at 9° and 21° [54,55]. On the other hand, the XRD of the loaded microparticles did not show any defined peak corresponding to crystalline MN. Although some peaks in the microparticulated systems such as 15.59° and 20.80° could correspond to MN, their intensity is in the range of the noise of the used instrument. This is in concordance with the results obtained by DSC analysis, confirming that MN is in an amorphous state, or that in the microparticles, the MN crystallinity was below the detection limit [56].

Halo Zone Test

As was observed in Fig. 8, after 1 h of assay, the halos produced by MN and the systems based on GEL and HPMC-GEL were the greatest (44–47 mm) showing significant

Table II. Tm Obtained from DSC Experiments for All the Studied Systems

Sample	Loaded MPs Tm (°C)	Empty MPs Tm (°C)
CH	180.1	177.3
HPMC	188.7	187.6
GEL	188.3	192.6
CH-HPMC	176.8	177.3
CH-GEL	186.1	178.2
HPMC-GEL	191.5	194.7

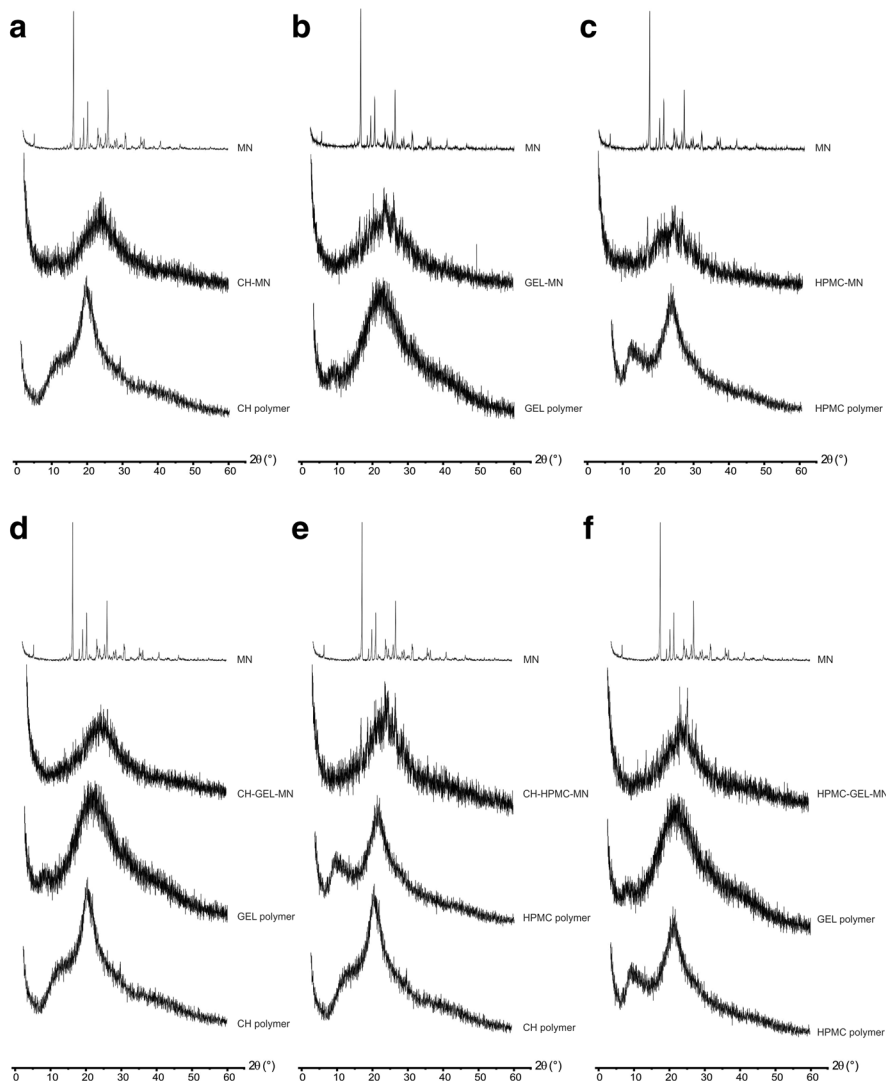*MPs*, microparticles; *Tm*, melting temperature

Fig. 7. **a–f** X-ray patterns of MN raw material, polymers, and different formulations
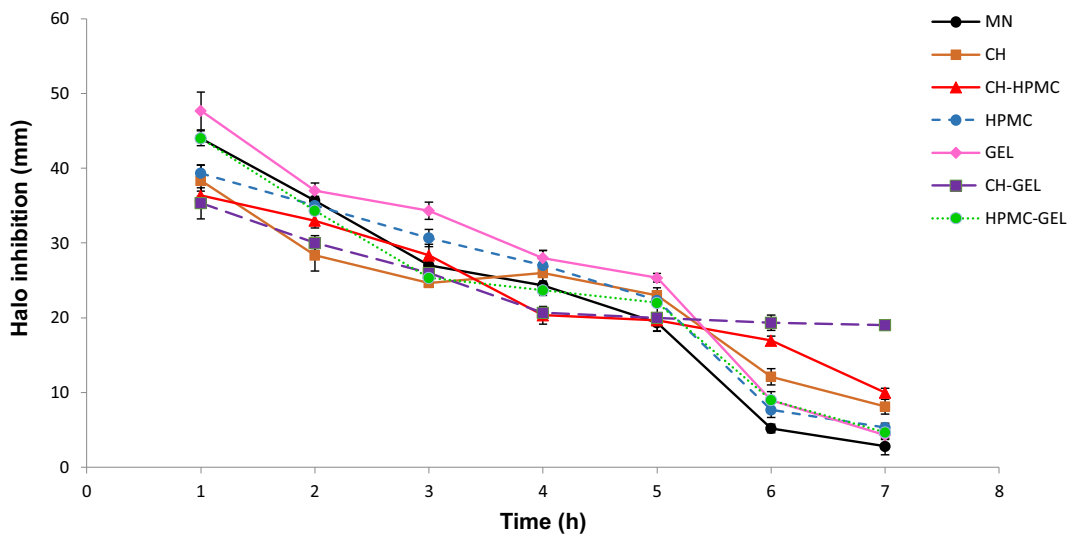

Fig. 8. Inhibition halos produced by MN and microparticulated systems

differences ($p < 0.05$) to other microparticulated systems (35–39 mm). At the second hour, significant differences ($p < 0.05$) were observed between the halos produced by microparticles based on CH and CH-HPMC (28–30 mm) with respect to the other systems (33–37 mm).

After 5 h of assay, halos produced by the MN raw material decreased significantly compared to all the systems, followed by microparticles based on GEL, HPMC, and combination of HPMC-GEL. Systems based on CH-HPMC and CH-GEL were able to produce greater inhibition halos after 6 and 7 h of assay. Particularly, the inhibition halo produced by the microparticles based on CH-GEL was maintained from the fourth- to the seventh-hour assay. These results could be explained by the exposure of MN to the culture medium. GEL is a hydrophilic polymer which easily swells in water exposing the MN loaded to the culture medium. On the other hand, CH is soluble in acid solutions but poorly swell in water, maintaining its microparticulate structure. After 1 h assay, microparticles, based on polymers which easily swell (GEL and HPMC-GEL), exposed more MN to the medium producing the highest halos. The microparticles based on CH produced smaller halos at the beginning of the assay, because the matrix was unable to swell in the medium, and therefore, a lower content of MN was exposed to the culture. However, halos around 20 mm were observed after 7 h of assay, while the MN raw material produced a smaller halo (3 mm). At this point, the MN halo was closer to that produced by the microparticles based on GEL. Thus, these results showed that the microencapsulation of MN in the CH-GEL matrix produced sustained and controlled release for this drug.

CONCLUSIONS

Different microparticulated systems based on combinations of natural cationic, anionic, and nonionic polymers loaded with miconazole nitrate were developed and characterized. All systems showed good encapsulation efficacies; among them, the higher values were obtained using ionic polymers probably due to the interactions between the drug and polymers before the spray drying process. The interactions between polymers were observed by IR, while the state of the drug and polymers in the systems was studied by TGA, DTGA, and DSC showing that polymers produce a protective effect on the drug and also that the drug is mainly in the amorphous state phase which was confirmed by XRD.

The *in vitro* activity of systems analyzed by the halo zone test experiment showed that composited microparticles based on oppositely charged polymers presented a controlled release of the drug, which improves its activity at prolonged time. This microparticulated formulation based on chitosan and gelatin and loaded with miconazole nitrate should be taken into account for further evaluation of its safety and *in vivo* efficacy to be considered as an alternative therapeutic system for the treatment of oral candidiasis.

FUNDING INFORMATION

REFERENCES

1. Spampinato C, Leonardi D. Candida infections, causes, targets, and resistance mechanisms: traditional and alternative antifungal agents. Biomed Res Int. 2013:1–13.
2. Dongari-Bagtzoglou A, Dwivedi P, Ioannidou E, Shaqman M, Hull D, Burleson J. Oral Candida infection and colonization in solid organ transplant recipients. Mol Oral Microbiol. 2009;24(3):249–54.
3. Andrés F, Klein T, Amanda L, Amanda M, Farago PV, Campanha NH. Development and validation of an RP-HPLC/UV method for determination of miconazole nitrate in spray-dried polymeric microparticles. Lat Am J Pharm. 2016;35(6):1354–60.
4. Abruzzo A, Cerchiara T, Bigucci F, Gallucci MC, Luppi B. Mucoadhesive buccal tablets based on chitosan/gelatin microparticles for delivery of propranolol hydrochloride. J Pharm Sci. 2015;104(12):4365–72.
5. Tejada G, Barrera MG, Piccirilli GN, Sortino M, Frattini A, Salomón CJ, et al. Development and evaluation of buccal films based on chitosan for the potential treatment of oral candidiasis. AAPS PharmSciTech. 2017;18(4):936–46.
6. Tejada G, Piccirilli GN, Sortino M, Salomón CJ, Lamas MC, Leonardi D. Formulation and in-vitro efficacy of antifungal mucoadhesive polymeric matrices for the delivery of miconazole nitrate. Mater Sci Eng C. 2017;79(Supplement C):140–50.
7. Mura P, Cirri M, Mennini N, Casella G, Maestrelli F. Polymeric mucoadhesive tablets for topical or systemic buccal delivery of clonazepam: effect of cyclodextrin complexation. Carbohydrate Polymers. 2016;152(Supplement C):755–63.
8. Alqurshi A, Kumar Z, McDonald R, Strang J, Buanz A, Ahmed S, et al. Amorphous formulation and in vitro performance testing of instantly disintegrating buccal tablets for the emergency delivery of naloxone. Mol Pharm. 2016;13(5):1688–98.
9. Sander C, Madsen KD, Hyrup B, Nielsen HM, Rantanen J, Jacobsen J. Characterization of spray dried bioadhesive metformin microparticles for oromucosal administration. Eur J Pharm Biopharm. 2013;85(3, Part A):682–8.
10. Nerkar P, Gattani S. Spray-dried buccal mucoadhesive microparticles of venlafaxine based on cress seed mucilage: in vitro, in vivo evaluation in rabbits. Dry Technol. 2012;30(9):968–78.
11. Keegan GM, Smart JD, Ingram MJ, Barnes L-M, Burnett GR, Rees GD. Chitosan microparticles for the controlled delivery of fluoride. J Dent. 2012;40(3):229–40.
12. Gad HA, Kamel AO, Ezzat OM, El Dessouky HF, Sammour OA. Doxycycline hydrochloride-metronidazole solid lipid microparticles gels for treatment of periodontitis: development, in-vitro and in-vivo clinical evaluation. Expert Opinion on Drug Delivery. 2017;14(11):1241–51.
13. Monajjemzadeh F, Gholizadeh N, Yousefzadeh Mobaraki N, Jelvehgari M. Physicochemical and in vitro mucoadhesive properties of microparticles/discs of betamethasone for the management of oral lichen planus. Pharm Dev Technol. 2016;21(8):996–1005.
14. Cartagena AF, Lyra A, Kapuchczinski AC, Urban AM, Esmerino LA, Klein T, et al. Miconazole nitrate-loaded microparticles for buccal use: immediate drug release and antifungal effect. Current Drug Delivery. 2016;14(8):1144–53.
15. Cartagena AF, Esmerino LA, Polak-Junior R, Olivieri Parreiras S, Domingos Michél M, Farago PV, et al. New denture adhesive containing miconazole nitrate polymeric microparticles: antifungal, adhesive force and toxicity properties. Dent Mater. 2017;33(2):e53–61.
16. Gierszewska M, Ostrowska-Czubenko J, Chrzanowska E. pH-responsive chitosan/alginate polyelectrolyte complex membranes reinforced by tripolyphosphate. Eur Polym J. 2018;101:282–90.
17. Tayel AA, Moussa S, El-Tras WF, Knittel D, Opwis K, Schollmeyer E. Anticandidal action of fungal chitosan against Candida albicans. Int J Biol Macromol. 2010;47(4):454–7.

18. Mati-Baouche N, Elchinger P-H, de Baynast H, Pierre G, Delattre C, Michaud P. Chitosan as an adhesive. Eur Polym J. 2014;60:198–212.

19. Garcia A, Leonardi D, Piccirilli GN, Mamprin ME, Olivieri AC, Lamas MC. Spray drying formulation of albendazole microspheres by experimental design. In vitro-in vivo studies. Drug Dev Ind Pharm. 2015;41(2):244–52.

20. García A, Barrera MG, Piccirilli G, Vasconi MD, Di Masso RJ, Leonardi D, et al. Novel albendazole formulations given during the intestinal phase of Trichinella spiralis infection reduce effectively parasitic muscle burden in mice. Parasitol Int. 2013;62(6):568–70.

21. Cigu TA, Vasiliu S, Racovita S, Lionte C, Sunel V, Popa M, et al. Adsorption and release studies of new cephalosporin from chitosan-g-poly(glycidyl methacrylate) microparticles. Eur Polym J. 2016;82:132–52.

22. Vasiliu S, Popa M, Luca C. Evaluation of retention and release processes of two antibiotics from the biocompatible core-shell microparticles. Eur Polym J. 2008;44(11):3894–8.

23. Khlibsuwan R, Siepmann F, Siepmann J, Pongjanyakul T. Chitosan-clay nanocomposite microparticles for controlled drug delivery: effects of the MAS content and TPP crosslinking. Journal of Drug Delivery Science and Technology. 2017;40(Supplement C):1–10.

24. Yu C-Y, Yin B-C, Zhang W, Cheng S-X, Zhang X-Z, Zhuo R-X. Composite microparticle drug delivery systems based on chitosan, alginate and pectin with improved pH-sensitive drug release property. Colloids Surf B: Biointerfaces. 2009;68(2):245–9.

25. Chowdary K, Rao YS. Design and in vitro and in vivo evaluation of mucoadhesive microcapsules of glipizide for oral controlled release: a technical note. AAPS PharmSciTech. 2003;4(3):87–92.

26. Campos E, Branquinho J, Carreira AS, Carvalho A, Coimbra P, Ferreira P, et al. Designing polymeric microparticles for biomedical and industrial applications. Eur Polym J. 2013;49(8):2005–21.

27. Mahmoudian M, Ganji F. Vancomycin-loaded HPMC microparticles embedded within injectable thermosensitive chitosan hydrogels. Progress in Biomaterials. 2017;6:49–56.

28. Kwon K, Kim J-C. Preparation of microparticles composed of cinnamoyl gelatin and cinnamoyl alginate by spray-drying method and effect of UV irradiation and pH value on their release property. J Dispers Sci Technol. 2017;38(2):187–93.

29. Alburquenque C, Bucarey SA, Neira-Carrillo A, Urzúa B, Hermosilla G, Tapia CV. Antifungal activity of low molecular weight chitosan against clinical isolates of Candida spp. Med Mycol. 2010;48(8):1018–23.

30. Elsabee MZ, Abdou ES. Chitosan based edible films and coatings: a review. Mater Sci Eng C. 2013;33(4):1819–41.

31. Hausberger AG, DeLuca PP. Characterization of biodegradable poly (D, L-lactide-co-glycolide) polymers and microspheres. J Pharm Biomed Anal. 1995;13(6):747–60.

32. Singh S, Jain S, Muthu M, Tiwari S, Tilak R. Preparation and evaluation of buccal bioadhesive films containing clotrimazole. AAPS PharmSciTech. 2008;9(2):660–7.

33. Shidhaye SS, Saindane NS, Sutar S, Kadam V. Mucoadhesive bilayered patches for administration of sumatriptan succinate. AAPS PharmSciTech. 2008;9(3):909–16.

34. Patel VF, Liu F, Brown MB. Modeling the oral cavity: in vitro and in vivo evaluations of buccal drug delivery systems. J Control Release. 2012;161(3):746–56.

35. Priotti J, Codina AV, Leonardi D, Vasconi MD, Hinrichsen LI, Lamas MC. Albendazole microcrystal formulations based on chitosan and cellulose derivatives: physicochemical characterization and in vitro parasiticidal activity in Trichinella spiralis adult worms. AAPS PharmSciTech. 2017;18(4):947–56.

36. Clinical and Laboratory Standards Institute W, PA. Method for antifungal disk diffusion susceptibility testing of yeasts. Approved guideline. Second edition. Document M44-A2. 2008.

37. Yeo Y, Park K. Control of encapsulation efficiency and initial burst in polymeric microparticle systems. Arch Pharm Res. 2004;27(1):1–12.

38. Craig DQ. The mechanisms of drug release from solid dispersions in water-soluble polymers. Int J Pharm. 2002;231(2):131–44.

39. Kumar CG, Poornachandra Y. Biodirected synthesis of miconazole-conjugated bacterial silver nanoparticles and their application as antifungal agents and drug delivery vehicles. Colloids Surf B: Biointerfaces. 2015;125(Supplement C):110–9.

40. Ribeiro A, Figueiras A, Santos D, Veiga F. Preparation and solid-state characterization of inclusion complexes formed between miconazole and methyl-β-cyclodextrin. AAPS PharmSciTech. 2008;9(4):1102–9.

41. Real DA, Martinez MV, Frattini A, Soazo M, Luque AG, Biasoli MS, et al. Design, characterization, and in vitro evaluation of antifungal polymeric films. AAPS PharmSciTech. 2013;14(1):64–73.

42. Park S-H, Chun M-K, Choi H-K. Preparation of an extended-release matrix tablet using chitosan/carbopol interpolymer complex. Int J Pharm. 2008;347(1):39–44.

43. de Britto D, Campana-Filho SP. A kinetic study on the thermal degradation of N,N,N-trimethylchitosan. Polymer Degradation and Stability. 2004;84(2):353–61.

44. Mainardes RM, Gremião MPD, Evangelista RC. Thermoanalytical study of praziquantel-loaded PLGA nanoparticles. Revista Brasileira de Ciências Farmacêuticas. 2006;42(4):523–30.

45. Li XG, Huang MR, Bai H. Thermal decomposition of cellulose ethers. J Appl Polym Sci. 1999;73(14):2927–36.

46. Ling WC. Thermal degradation of gelatin as applied to processing of gel mass. J Pharm Sci. 1978;67(2):218–23.

47. Dranca I, Vyazovkin S. Thermal stability of gelatin gels: effect of preparation conditions on the activation energy barrier to melting. Polymer. 2009;50(20):4859–67.

48. Chen CH, Wang FY, Mao CF, Yang CH. Studies of chitosan. I. Preparation and characterization of chitosan/poly (vinyl alcohol) blend films. J Appl Polym Sci. 2007;105(3):1086–92.

49. Chavan RB, Thipparaboina R, Kumar D, Shastri NR. Evaluation of the inhibitory potential of HPMC, PVP and HPC polymers on nucleation and crystal growth. RSC Adv. 2016;6(81):77569–76.

50. Eldridge JE, Ferry JD. Studies of the cross-linking process in gelatin gels. III. Dependence of melting point on concentration and molecular weight. J Phys Chem. 1954;58(11):992–5.

51. Blasi P, Schoubben A, Giovagnoli S, Perioli L, Ricci M, Rossi C. Ketoprofen poly (lactide-co-glycolide) physical interaction. AAPS PharmSciTech. 2007;8(2):E78–85.

52. Li X, Xie H, Lin J, Xie W, Ma X. Characterization and biodegradation of chitosan–alginate polyelectrolyte complexes. Polym Degrad Stab. 2009;94(1):1–6.

53. Dong Z, Wang Q, Du Y. Alginate/gelatin blend films and their properties for drug controlled release. J Membr Sci. 2006;280(1–2):37–44.

54. Wang L, Dong W, Xu Y. Synthesis and characterization of hydroxypropyl methylcellulose and ethyl acrylate graft copolymers. Carbohydr Polym. 2007;68(4):626–36.

55. Nart V, Franca MT, Anzilaggo D, Riekes MK, Kratz JM, de Campos CEM, et al. Ball-milled solid dispersions of BCS class IV drugs: impact on the dissolution rate and intestinal permeability of acyclovir. Mater Sci Eng C. 2015;53:229–38.

56. Leuner C, Dressman J. Improving drug solubility for oral delivery using solid dispersions. Eur J Pharm Biopharm. 2000;50(1):47–60.